International Journal for Parasitology: Parasites and Wildlife 23 (2024) 100920

Contents lists available at ScienceDirect

International Journal for Parasitology: Parasites and Wildlife

journal homepage: www.elsevier.com/locate/ijppaw

A new species of *Demodex* (Acari: Demodecidae) from the skin of golden-handed tamarins, *Saguinus midas* (Primates: Cebidae)

Toshihiro Tokiwa [a,*], Kengo Ueda [b,c], Nagi Watanabe [a], Shyun Chou [a], Kiyokazu Ozaki [c]

[a] *Laboratory of Veterinary Parasitology, Nippon Veterinary and Life Science University, 1-7-1 Kyonancho, Musashino, Tokyo, Japan*
[b] *Vogel Animal Hospital, 5-1-1 Kotoku-cho, Nada, Kobe, Hyogo, Japan*
[c] *Laboratory of Pathology, Setsunan University, 45-1 Nagaotoge-cho, Hirakata, Osaka, Japan*

ARTICLE INFO

Keywords:
Demodex midae n. sp.
Demodectic mange
Fluralaner: golden-handed tamarin
Histopathology
Sequence analysis

ABSTRACT

Two captive-bred golden-handed tamarins, *Saguinus midas* L., 1758 (Primates: Cebidae), kept in households in Japan, presented with psoriasis-like plaques on their faces, along with scale, alopecia, and itching. Histopathological examination revealed numerous *Demodex* mites in the hair follicles, and the clinical symptoms in both cases improved after treatment with fluralaner. Based on the morphological and genetic characteristics of the mites collected from tamarins, we describe a new species of *Demodex*. This new species is the fifth valid *Demodex* species recorded from primates.

1. Introduction

Demodectic mange is a cutaneous disease observed in domestic and wild animals and primates, including humans. It is caused by infection of demodecid mites of the family Demodecidae and only four valid *Demodex* species have been described in primates (Nutting, 1964; Lebel and Nutting, 1973; Karjala et al., 2005; Izdebska and Rolbiecki, 2020); *Demodex brevis* Akbulatova, 1963 and *Demodex folliculorum* (Simon, 1842) from human, *Demodex macaci* Karjala et al., 2005 from rhesus monkey (*Macaca mulatta*), and *Demodex saimiri* Lebel and Nutting, 1973 from common squirrel monkey (*Saimiri sciures*).

Infection with demodecid mites is often subclinical but can be severe depending on the age and immune status of the host. Although five cases of demodectic mange have been reported in tamarins of the genus *Saguinus* (Primates: Cebidae: Callitrichinae) (Hickey et al., 1983; James and Raphael, 2000; Churgin et al., 2018), New World monkeys native to South America (Brcko et al., 2022), the morphological and genetic characteristics of *Demodex* mites from tamarins have not yet been investigated. In the present study, two cases of demodectic mange due to infection with *Demodex* species in two captive-bred golden-handed tamarins (*Saguinus midas*) were reported, along with histopathological and parasitological findings and treatment history. The obtained *Demodex* mite from tamarins is considered an undescribed species based on morphological and genetic characteristics and host species and is therefore proposed as a new species in this report.

2. Materials and methods

2.1. Case presentation

Two imported captive-bred golden-handed tamarins from one household in Osaka, Japan, presented with psoriasis-like plaques and alopecia on their heads in 2021. These unrelated tamarins were obtained from different facilities but were kept together for breeding purposes. The dates of import into Japan and the country of export were unknown. Several lesser bushbabies (*Galago senegalensis*) (Primates: Galagidae) were kept by the same owner.

The first case (case 1) was a female and purchased from a pet shop in Japan in 2018. In August 2020, the monkey gave birth to two pups, but there was no abnormalities at this point. In January 2021, the owner noticed that the back of the nose was dry along with scale. Skin lesions gradually worsened and spread to the auricular region. The owner gave up on taking the tamarin to the hospital because of their rough nature and the difficulty in holding them. In April 2021, the tamarin was brought to the hospital for the first time. The tamarin weighed 485 g, and the lesions extended from the face to the temporal region, especially on the right temple, showing severe psoriasis-like plaques with hair loss and scale (Fig. 1A and B). The skin lesion was biopsied using a disposable 4-mm punch under general isoflurane anesthesia.

The second tamarin (case 2) was a male cage mate of case 1 and was purchased at a different pet shop by the same owner approximately 5

* Corresponding author. Laboratory of Veterinary Parasitology, Nippon Veterinary and Life Science University, Japan.
E-mail address: tokiwa@nvlu.ac.jp (T. Tokiwa).

https://doi.org/10.1016/j.ijppaw.2024.100920
Received 11 January 2024; Received in revised form 1 March 2024; Accepted 1 March 2024
Available online 2 March 2024
2213-2244/© 2024 The Authors. Published by Elsevier Ltd on behalf of Australian Society for Parasitology. This is an open access article under the CC BY-NC-ND license (http://creativecommons.org/licenses/by-nc-nd/4.0/).

months prior to case 1. A few days after purchase, the owner noticed dandruff on the face, but it was left untreated. On May 18, 2021, the tamarin was brought to the hospital for the first time, complaining of skin lesions similar to those in case 1. The tamarin weighed 465 g. Physical examination under general anesthesia revealed mild hair loss in the temples. Demodecid mites were detected during the skin scraping test, and the lesion was biopsied using the same procedure as in case 1.

In June 2021, based on the detection of demodecid mites by skin biopsy or scratch examinations, both monkeys received a single oral administration of half Bravecto® A Tablet (MSD Animal Health, Japan), which delivers 15 mg/kg as a fluralaner. No adverse effects were observed after the administration of fluralaner. Physical examination under general anesthesia with isoflurane, approximately 5 months after administration, revealed reduced itching, disappearance of scale, and hair growth (Fig. 1C and D) in both cases.

2.2. Histopathological examination

Histopathological examination of the tissue biopsy in case 1 was performed at Setsunan University. The tissues fixed in 10% neutral-buffered formalin were routinely processed and embedded in paraffin. Sections of 4 μm-thick were then stained with hematoxylin and eosin (H&E). The mitotic count was obtained by counting the number of mitotic figures in 10 consecutive microscopic high-power fields (HPFs) covering an area of 2.37 mm^2. We performed labeled-polymer immunohistochemistry using N-Histofine MAX PO (Nichirei Biosciences, Tokyo, Japan) with Iba-1, CD204, MHC-II, and MIB-1 as primary antibodies. The primary antibodies and methods used for immunohistochemistry are summarized in Table 1.

2.3. Detection of pathogens

Specimens were collected from the surface of the lesion in case 1 using sterile swabs and subjected to a commercial laboratory for bacterial and fungal culture and identification.

2.4. Morphological observation of demodecid mites

Microscopic examination of demodecid mites in the lesion was performed at Nippon Veterinary and Life Science University. Cryopreserved biopsied specimens from cases 1 and 2 were dissolved in 40% KOH solution, mounted on slides in Faure's medium and examined under a BX53 Nomarski differential interference contrast microscope (Olympus, Japan). Measurements were made with cellSens software (Olympus) and were reported in micrometers as holotype in brackets, followed by the mean and standard deviation, and the ranges in parentheses. Line drawing was conducted using FireAlpaca ver. 2.0 (https://firealpaca.com/ja/). The terminology for demodecid mites follows that described by Nutting (1976), Bochkov (2009), and Izdebska and Rolbiecki (2020).

2.5. Genetic analysis of mite

For molecular analyses, total genomic DNA was extracted from a single mite using the QIAamp DNA mini kit (Qiagen, Germany) according to the manufacturer's instructions, and used as a template for PCR analysis. Two genetic loci, nuclear 18S rDNA (18S, 527 bp) and mitochondrial 16S rDNA (16S, 292 bp), were amplified and sequenced using the primers listed in Table 2. PCR was performed using 20 μL reaction volumes, each containing 0.2 μL of TaKaRa Ex Taq (Takara Bio Inc., Japan), 2 μL of 10 × buffer, 1.6 μL of dNTPs (2.5 mM each), 0.2 μL of each primer (50 μM), 1.0 μL of the template, and 14.8 μL of double-distilled water. The amplification program consisted of initial denaturation at 95 °C for 2 min, followed by 35 (for 18S) or 30 (for 16S) cycles at 95 °C for 30 s, 52 °C for 30 s, and 72 °C for 30 s, with a final extension step at 72 °C for 4 min. The PCR products were analyzed by 1.5% agarose gel electrophoresis, purified with ExoSAP-IT (Thermo Fisher Scientific, USA), and sequenced with an Applied Biosystems 3730xl DNA analyzer (Applied Biosystems, USA) at Macrogen (Tokyo, Japan) using PCR primers.

Representative sequences have been deposited in the DNA Data Bank of Japan (DDBJ). Sequence similarity was determined using BLAST analysis from the National Center for Biotechnology Information

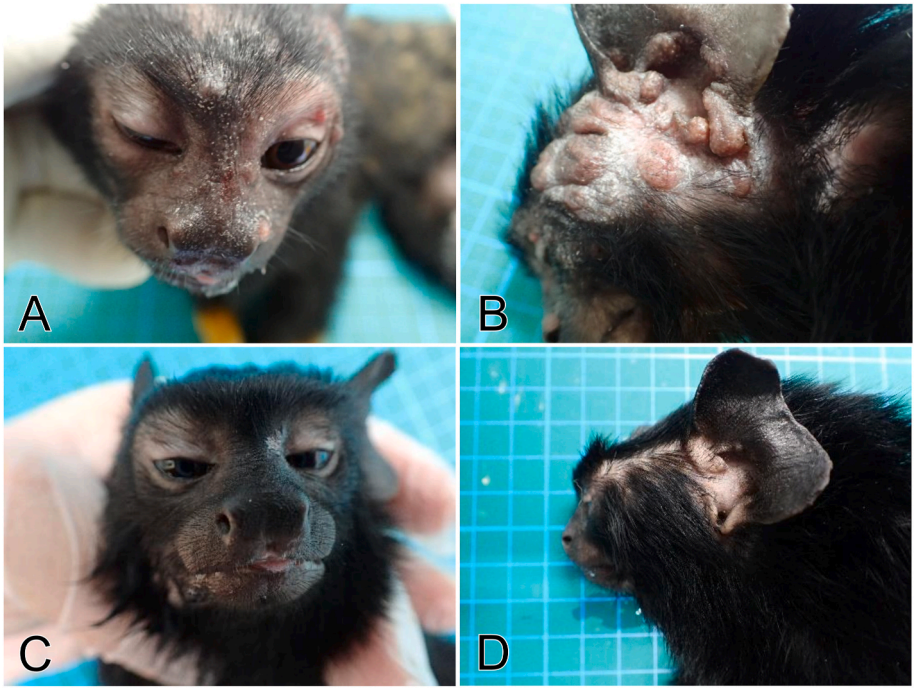

Fig. 1. Photographs of a male red-handed tamarin of case 1. (A and B) On initial examination, hair loss, and scale are found on the face, especially severe on the left temple, with numerous psoriasis-like plaques. (C and D) Findings of five months after treatment with fluralaner showing resolution of related lesions. (For interpretation of the references to colour in this figure legend, the reader is referred to the Web version of this article.)

Table 1
Primary antibodies and method used for immunohistochemistry, and immunohistochemical findings.

Antibody	Host (clone)	Dilution	Antigen retrieval method	Secondary antibody	Source	Positive rate (%) of round cells around follicle
Iba-1	rabbit polyclonal	1/250	HIER (citrate buffer, pH 6.0), pressure cooker	Simple stain (rabbit)	Wako, Osaka, Japan	100
CD204	mouse monoclonal (SRA-E5)	1/500	HIER (citrate buffer, pH 6.1), boilling	Simple stain (mouse)	Trans Genic, Fukuoka, Japan	10.0
MHC-II	mouse monoclonal (TAL.1B5)	1/100	HIER (citrate buffer, pH 6.2), microwave	Simple stain (mouse)	Dako, Glostrup, Denmark	0
Ki-67	mouse monoclonal (MIB-1)	1/100	HIER (citrate buffer, pH 6.0), pressure cooker	Simple stain (mouse)	Dako, Glostrup, Denmark	85.5

HIER, heat-induced epitope retrieval.

Table 2
Primers used in this study.

Primers	Gene	Direction	Sequence 5'to 3'	References
18S–F	18S	Forward	TCCAAGGAAGGCAGCAGGCA	Sastre et al. (2016)
18S–R	18S	Reverse	CGCGGTAGTTCGTCTTGCGACG	Sastre et al. (2016)
16S–F	16S	Forward	GTATTTTGACTGTGCTAAGGYAGC	Sastre et al. (2012)
16S–R	16S	Reverse	CAAAAGCCAACATCGAGG	Sastre et al. (2012)

website (https://blast.ncbi.nlm.nih.gov/Blast.cgi). Reference sequences for 18S and 16S were obtained from the DDBJ/ENA/GenBank databases. The sequences were aligned using the MAFFT online service with the option Q–INS–I setting (Katoh and Standley, 2013) and phylogenetic analysis was conducted on the 18S and 16S nucleotide sequences using Molecular Evolutionary Genetics Analysis (MEGA) software, version 11.0 (Tamura et al., 2021). The best-fitting substitution models were estimated based on the lowest Akaike information criterion values, and maximum likelihood (ML) phylogenetic trees were constructed based on the Tamura 3-parameter + G (18S) or Tamura-Nei + G + I (16S) substitution models. All positions containing gaps and missing data were eliminated. Bootstrap support for branching was based on 1000 replications.

3. Results

3.1. Laboratory diagnosis

In both cases, no potentially dermatopathogenic bacteria or fungi were detected in the cultures.

Histologically, the hair follicles were diffusely and markedly dilated up to 1 mm in diameter (Fig. 2). Numerous mites were observed within dilated follicles. In heavily infested and expanded hair follicles, the follicular epithelium was thin with no degeneration or necrosis. Infested hair follicles were surrounded by nodular monotonous macrophage/histiocyte infiltrates. The monotonously infiltrating macrophages/histiocytes were round to short spindle-shaped, with cell boundaries generally distinct and abundant in the eosinophilic cytoplasm. The nuclei were round to slightly irregular, with coarse granular chromatin and small nucleoli. The mitotic count was 16/10 HPFs, 2.37 mm^2. Immunohistochemically, these cells were strongly positive for Iba-1, slightly positive for CD204, and negative for MHC-II. The Ki-67 labeling index was 85.5%. Positive staining for Iba-1 and CD204 indicated that the round cells were derived from macrophages/histiocytes.

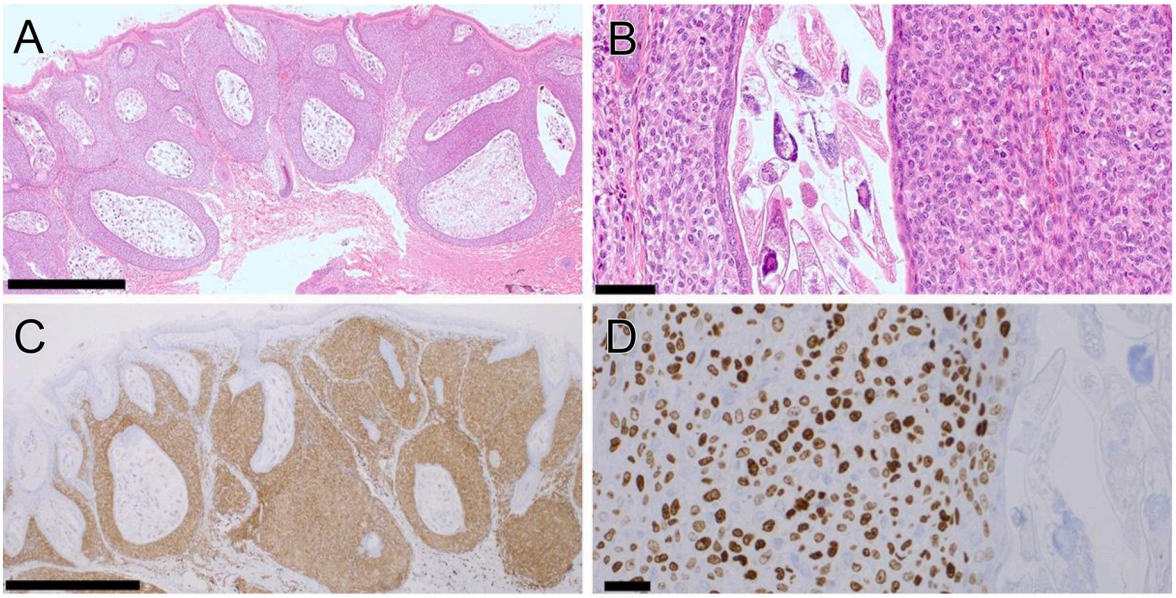

Fig. 2. Demodectic mange in a male golden-handed tamarin (case 1). (A) Macrophage/histiocyte accumulate and form nodules around the follicles that have filled and expanded with demodecid mites. H&E. Scale bar = 1 mm. (B) Dilated hair follicles are filled with transverse or cross sections of demodecid mites. The monotonous infiltrating macrophage/histiocyte surrounding the follicle has round to slightly irregular nuclei and abundant eosinophilic cytoplasm. Numerous mitotic figures are seen. H&E. Scale bar = 50 μm. (C) Almost all macrophage/histiocytes are strongly immunolabeled with Iba-1. Scale bar = 1 mm. (D) Numerous macrophage/histiocytes are immunolabeled for Ki-67 with a Ki-67 labeling index of 85.5%. Scale bar = 50 μm. (For interpretation of the references to colour in this figure legend, the reader is referred to the Web version of this article.)

Macrophages/histiocytes showed numerous mitotic figures and a high Ki-67 labeling index, but infiltration was not observed in the demodecid-free hair follicles, suggesting that growth was not neoplastic. Follicles without mites had no abnormalities and were not surrounded by histiocytes. Based on these results, the tamarin was histopathologically diagnosed with chronic granulomatous folliculitis and dermatitis with demodecid mite infection.

The demodecid mites detected in the skin tissues of both cases were males, females, and eggs of the same species, with only one deutonymph found, and no larvae detected. Based on morphological characteristics and comparison with other valid genera (Bochkov, 2009; Izdebska and Rolbiecki, 2020), the mite was identified as an undescribed *Demodex* species. The species is described based on males, females, and eggs as follows.

3.2. Description

Order Trombidiformes Reuter, 1909
Family Demodecidae Nicolet, 1855
Genus *Demodex* Owen, 1853
Demodex midae n. sp.

Male (n = 9 and a holotype) (Fig. 3A–F): Slender body, highly elongated; body length [Holotype = 146.5] 154.3 ± 6.9 (139.0–160.9); body length to width ratio [4.4] 5.1 ± 0.5 (4.4–5.9). Gnathosoma trapezoidal in outline; [16.2] 17.1 ± 0.9 (16.0–19.2) long and [20.4] 19.5 ± 1.2 (16.8–20.8) wide. Terminal-free segment of palp with two large, conical spines and 2 min, conical spines (Fig. 3A and C). Supracoxal spines (setae *elc.p*) (Fig. 3B and D), ca. [2.2] 2.3 (2.1–3.3) long, spaced [11.8] 11.6 ± 0.3 (11.0–12.0) apart; each spine bends in the midline. Subgnathosomal setae (setae *n*) [Fig. 3A] as faint dots lateral to the central margin of the horseshoe-shaped pharyngeal bulb and spaced

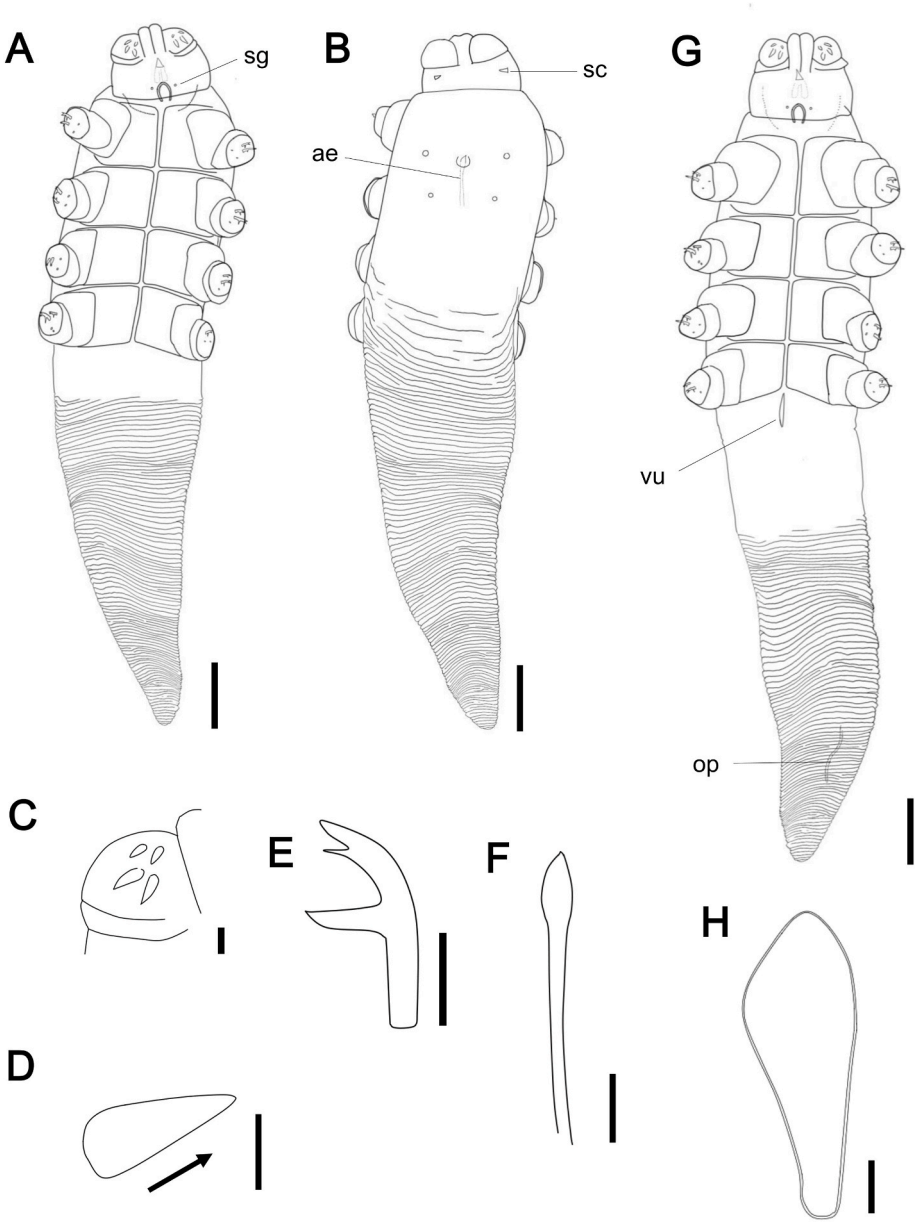

Fig. 3. *Demodex midae* n. sp. (A) Holotype male, ventral view. (B) Holotype male, dorsal view. (C) Spines on the right palpus, male, ventral view. (D) Supracoxal spine, male, dorsal view, arrows indicate the orientation of the left spine as a view on the gnathosoma. (E) Claw on the leg of tarsi, male. (F) Aedeagus. (G) Female, ventral view. (H) Egg. ae: aedeagus, op: opisthosomal organ, sg: subgnathosomal setae (setae *n*), sc: supracoxal spine (setae *elc.p*), vu: vulva. Scale bars = 20 μm (A, B, G, H) and 1 μm (C–F).

[3.5] 3.7 ± 0.4 (3.2–4.3) apart. Podosoma rectangular; [50.4] 51.6 ± 0.7 (50.4–52.5) long and [33.1] 30.4 ± 2.7 (25.4–33.5) wide; four pairs of five segmented short legs, with coxa integrated into ventral idiosomal wall; small interspaces separate epimeral plates (coxal fields) in the midline and aligned; pair coxa I triangular, and pairs II, III and VI trapezoidal. Tibiotarsus of each leg with a pair of forked claws (Fig. 3E), c.a. [2.0] (1.8–2.1), with large spur, and two knobs. Tarsus I and II, each with a minute dorsal solenidion. Aedeagus tubular (Fig. 3F), [8.5] 8.5 ± 0.7 (8.0–9.9) long, pointed apically with bulbous apical; genital opening on the dorsum at the level of the posterior margin of coxa I. Prodosal tubercles arranged in trapezoidal: interspace of first pairs [16.9] 16.8 ± 1.3 (15.0–19.5) long, of second pair [12.9] 15.4 ± 2.5 (12.0–19.8) long, distance between pairs [9.1] 8.5 ± 0.7 (7.8–9.5). Opisthosoma tubular, gradually tapered toward the end; [79.9] 85.5 ± 5.7 (73.0–91.0) long, represents [55%] 54% (52–57%) of the body. Opisthosoma distinctly annulated; annulations along its entire length on the dorsal side, but along its the posterior three-quarters to four-fifths on ventral side. Opisthosomal organs are absent.

Female (n = 14) (Fig. 3G): Slender body, highly elongated; body length 166.5 ± 21.3 (136.9–210.7); body length to width ratio 5.7 ± 1.1 (4.2–8.0). Gnathosoma as in male; 17.4 ± 1.4 (15.2–20.1) long and 20.2 ± 1.5 (16.5–22.1) width. Supracoxal setae (setae *elc.p*) as in male; spaced 12.1 ± 0.5 (11.6–12.7) apart. Subgnathosomal setae (setae *n*) as in male; spaced 4.7 ± 0.4 (4.2–5.2). Podosoma as in male; 52.6 ± 3.8 (43.3–58.9) long and 29.5 ± 2.9 (24.8–33.5). Prodorsal tubercles arranged tetrazoidal: interspace of fast pairs 20.2 ± 0.4 (19.7–20.7) long, of second pairs 22.5 ± 0.8 (21.4–23.6) long. Vulva a longitudinal slit, 4.7 ± 0.4 (4.2–5.2) long, anterior limit commences just behind the median confluence of coxal plates IV. Opisthosoma as in male; 96.3 ± 19.5 (67.3–133.2) long, constitutes 57% (48–65%) of body length. Opisthosoma distinctly annulated; annulations along its entire length on the dorsal side, but along its the posterior two-thirds on ventral side. The pore of the linear opisthosomal organ, located in the posterior part of the opisthosoma, is long anterior to the opisthosomal terminus.

Egg (n = 15) (Fig. 3H): Spindle-shaped with asymmetry in the major axis and bluntly rounded ends; 77.5 ± 3.1 (72.7–83.6) long and 24.0 ± 1.2 (21.3–25.2) wide. The chorion smooth; without operculum.

Type host: *Saguinus midas* L., 1758 (Primates: Cebidae).

Habitat: Hair follicles on the face of the host. Other body parts were not examined.

Etymology: The specific epithet "*midae*" is adopted from the specific name of the type host.

Material deposited: The slides containing holotype male (MPM Coll. No. 25276) and paratypes (MPM Coll. No. 25277) were deposited in the Meguro Parasitological Museum, Meguro, Tokyo, Japan. Representative sequences were deposited in the DNA Data Bank of Japan (18S: accession nos. LC796752; 16S: accession no. LC796753).

ZooBank registration number: 7B16AD86-C203-45FE-B70C-B95BAA8022DB.

Remarks: *Demodex midae* n. sp. from golden-handed tamarins is morphologically most similar to *D. macaci* from the rhesus monkey (*Macaca mulatta*) (Karjala et al., 2005). However, total length of female and aedeagus of male of *D. midae* n. sp. are shorter than those of *D. macaci* (Table 3). *Demodex midae* n. sp. has two large and two small spines on the palp, while *D. macaci* has four small spines. Male genital opening on the dorsum at the level of the posterior margin of legs I in *D. midae* n. sp., while in *D. macaci* it on anterior margin of legs II.

3.3. Sequence analyses of Demodex midae n sp.

The partial 18S sequence of *D. midae* n. sp. (527 bp) showed 92.5%–97.0% identities with *Demodex* spp., and the highest homology was found with *D. ursi* (accession no. KC010482) from the black bear (*Ursus americanus*) and *D. musculi* (accession no. JF834894) from house mouse (*Mus musculus*) and *Demodex* sp. from white-tailed deer (*Odocoileus virginianus*) (accession no. KC010483). The identity of *Demodex* species

Table 3
Morphometric comparison of features (as means) of *Demodex midae* n. sp. and *Demodex macaci*.

	D. midae n. sp.		*D. macaci*	
	Males (n = 10)	Females (n = 14)	Males (n = 20)	Females (n = 20)
Body total L	154.3	166.5	149	213
Body total W	30.4	29.5	27	31
Body L/W ratio	5.1	5.7	5.5	6.8*
Opisthosoma L to body L ratio (%)	55	57	60	65
Aedeagus L	8.5	–	16	–
Vulva L	–	4.7	–	5
Egg L	–	77.5	–	78
References	Present study		Karjala et al. (2005)	

L: length, W: width, Asterisk: calculated from the mean value.

parasitic on primates was less than 96.6% for *D. folliculorum* and 93.7% for *D. brevis*. No other sequences detected from primates were available. In the ML tree based on 18S sequences, with *Myobia* (Trombidiformes: Prostigmata: Myobiidae) as an outgroup (Fig. 4A), *Demodex* spp. (Trombidiformes: Cheyletoidea: Demodecidae) formed a monophyletic group that was well-separated from *Cheletomimus* and *Neochelacheles* (Trombidiformes: Cheyletoidea: Cheyletidae). Within the *Demodex* clade, *D. folliculorum, D. canis,* and *D. injai* formed a monophyletic clade with relatively high bootstrap values (>74%). *Demodex* species derived from the same host (*D. folliculorum* and *D. brevis* in humans, *D. canis* and *D. injai* in dogs) were polyphyletic, except for feline *D. cati*, *D. gatoi,* and *Demodex* sp. However, the phylogenetic relationships among these groups and other *Demodex* species, including *D. midae* n. sp. were not clear.

The 16S sequence of *D. midae* n. sp. (292 bp) showed 75.0%–84.5% homology with *Demodex* spp., and the highest homology was found with *D. folliculorum* (accession no. KF875587). In the midpoint-rooted ML tree based on 16S sequences (Fig. 4B), human *D. folliculorum* and canine *D. injai*, and human *D. brevis* and feline *D. gatoi* showed monophyletic groups, respectively. Although *D. midae* n. sp. is distinguishable from other *Demodex* species/isolates, its phylogenetic relationship with these species is unclear.

4. Discussion

Several studies have used 18S and 16S sequences for the molecular identification of *Demodex* species from humans or canines (Sastre et al., 2012, 2016; Thoemmes et al., 2014; Palopoli et al., 2015; Prasher et al., 2020). In this study, we conducted phylogenetic analyses using the 18S and 16S sequences of *Demodex* spp. from different hosts. Both sequences of *D. midae* n. sp. were clearly distinguishable from those of other *Demodex* species from humans (*D. folliculorum* and *D. brevis*), dogs (*D. canis* and *D. injai*), cats (*D. cati* and *D. gatoi*), and other *Demodex* species/isolates available in the database. These results indicated that the 18S and 16S seuqences of *D. midae* n. sp. are useful genetic markers for identification at the genus and species levels. However, the details of the phylogenetic relationships among *Demodex* species/isolates have not been clarified using single-locus analysis.

Demodex mites are generally recognized as strictly host-specific, and each primate has its unique fauna (Izdebska and Rolbiecki, 2020), and thus, *Demodex* mites are transmitted via contact with the same host species. Horizontal transmission was suspected in previous and present cases of tamarins (Table 4), as has been observed in cagemates or siblings. To date, six *Demodex* spp. have been recorded in primates. In this group, *D. folliculorum* and *D. brevis* are specific to humans. Of the four remaining species, *D. sciurei* detected in the common squirrel monkey (*Saimiri sciureus*) (Cebiada) (Lebel, 1970) and *D. araneae* detected in the spider monkey (*Ateles* sp.) (Atelidae) (Nutting, 1950, 1964) are considered *nomina nuda*, as they have not been formally described and

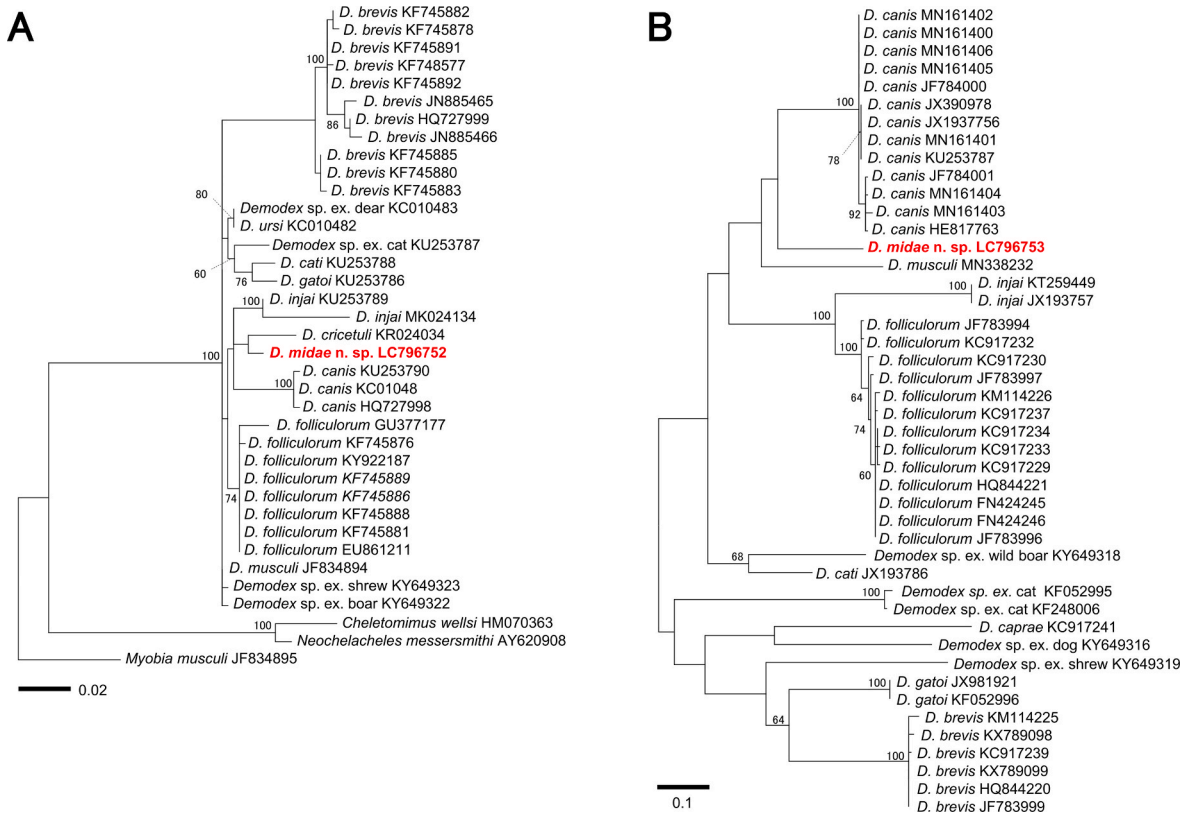

Fig. 4. Maximum likelihood phylogenetic trees of *Demodex* (Trombidiformes: Cheyletoidea: Demodecidae). (A) 18S sequence-based rooted phylogenetic tree with *Myobia* (Trombidiformes: Prostigmata: Myobiidae) as outgroup and *Cheletomimus* and *Neochelacheles* (Trombidiformes: Cheyletoidea: Cheyletidae) as related species of *Demodex*. (B) 16S sequence-based midpoint-rooting tree. Accession numbers are shown in roman next to the taxa names. Nodes are labeled with bootstrap values greater than 60%. Scale bars represent substitutions per site.

Table 4
Clinicopathological data of demodectic mange reported from *Saguinus* spp. (Primates: Cebidae: Callitrichinae).

Host	*S. geoffroyi*	*S. midas*	*S. midas*	*S. midas*
Locality	USA	USA	Hong Kong	Japan
Sex (age)	F (Young)	M (5 y.o.) and F (2 y.o.)	M (2 y.o.) and F (2 y.o.)	M (Adult) and F (Adult)
Relationships	–	Cage mate	Sibling	Cage mate
Site of lesions	Extremities, tail head	Face, extremities	Face, trunk, extremities	Face
Lesions and symptoms	Erythematous and covered with papules ranging from pinpoint to 3 mm in diameter; Mild alopecia	Diffuse, multifocal, raised, firm, nonpruritic, hyperkeratotic lesion	Multiple raised, Plaque-like lesions; weight loss	Multiple raised, Plaque-like lesions; scales
Stage of *Demodex* [Morphological characteristics]	Adult [N.A.]	Adult [N.A.]	Adult [cigar shape. 175–182.5 μm in length], Egg [N.A.]	Adult, deutonymph, egg [See description]
Successful treatment [Adverse effect]	Spontaneous remission [N.A.]	Repeated Amitraz (125 ppm) dipping for 2–5 min [Ataxia for about 3 days after treatment]	Fluralaner (30–35 mg/kg), once a day, p.o. as tablet [N.A.]	Fluralaner (15 mg/kg), once a day, p.o. as tablet [N.A.]
Other animals kept in the facility	Small colony of *S. geoffroyi*	N.A.	Capybaras (*Hydrochoerus hydrochaeris*)	Lesser bushbabys (*Galago senegalensis*)
References	Hickey et al. (1983)	James and Raphael (2000)	Churgin et al. (2018)	This study

M: male, F: female, y.o.: years old, N.A.: Not available or not stated, p.o.: oral administration.

are included in an unpublished dissertation (Izdebska and Rolbiecki, 2020). In addition to these species, undescribed demodecid mites have been documented from golden lion tamarin (*Leontopithecus rosalia*) (Wilson et al., 1989), golden-handed tamarin (*Saguinus midas*) (James and Raphael, 2000; Churgin et al., 2018), Geoffroy's tamarin (*Saguinus geoffroyi*) (Hickey et al., 1983), common woolly monkey (*Lagothrix lagotricha*) (Peddie and Larson, 1971), northern night monkey (*Aotus trivirtatus*) (Lebel and Nutting, 1973), Goeldi's monkey (*Callimico goeldii*) (Gruber-Dujardin et al., 2019), chimpanzee (*Pan troglodyes*) (Phillipe, 1948), and Senegal bushbaby (*Galago senegalensis*) (Kuznetsova et al., 2012). These reports mainly focused on the clinical course and lesions, and it was not possible to compare these mites because their detailed morphological and genetic characteristics have not been described. However, the microphotograph of *Demodex* sp. reported from golden-handed tamarins (Churgin et al., 2018), appeared similar to *D. midae* n. sp. In contrast, the morphological characteristics of *D. midae* n. sp. were different from those of *Demodex* sp. reported in Geoffroy's tamarins, which has short body (Hickey et al., 1983). These results suggest that the species of *Demodex* may differ depending on the *Saguinus* species and that there may be additional undescribed species in other primates.

In primates, human demodectic mange is well-known and can be

divided into primary and secondary clinical forms (Chen and Plewig, 2014). The primary form has no known cause but occurs mainly in the elderly population, where mites multiply on the face, and treatment requires appropriate acaricides, such as ivermectin, permethrin, crotamiton, lindane, benzyl benzoate, and pilocarpine. The secondary forms occur in patients with immunosuppression or other skin diseases. Including this study, seven cases have been observed in *Saguinus* tamarins (Table 4). The gross lesions in the cases reported in this study are very similar to those seen in a previous report on captive-bred golden-handed tamarins from the USA (James and Raphael, 2000) and China (Churgin et al., 2018), and multiple plaque-like lesions with alopecia have been observed on the head. Histological findings are also similar to those of the demodectic mange of the golden-handed tamarin (Churgin et al., 2018), and nodular granulomatous inflammatory infiltrates surrounding dilated hair follicles. All cases resembled the primary forms of human demodectic mange because the tamarins were adults, had no underlying diseases, had lesions primarily on the face, and required antiectoparasitic administration for treatment.

James and Raphael (2000) reported that ivermectin inoculation did not improve demodectic mange in tamarins, and subsequent amitraz baths resulted in ataxia, whereas Churgin et al. (2018) reported that after a single oral dose of 30–35 mg/kg of fluranel, skin symptoms were alleviated and *Demodex* mites disappeared (Table 4). Fluralaner is a long-acting isozaline used in veterinary medicine that selectively inhibits chloride channels in arthropods such as fleas and ticks (Gassel, et al., 2014). It has recently been used to treat demodectic mange in dogs, cats, and golden hamsters (Perego et al., 2019; Duangkaew and Hoffman, 2018; Brosseau, 2020). In the present case, the skin symptoms of both tamarins were improved by a single fluralaner administration, and no adverse reactions were observed. Although fluralaner is not approved in Japan for the treatment of demodectic mange in non-human primates, these data indicate that fluralaner has the potential to treat demodectic mange in tamarins.

In conclusion, we report the clinical manifestations and treatment of demodectic mange in two captive-bred golden-handed tamarins and describe the pathogen that we detected as a new species of *D. midae* n. sp. Future studies on the prevalence of *D. midae* n. sp. in tamarins of wild and captive-bred populations and pathogenicity are required.

Ethical approval

Ethics approval was not required. Informed consent was obtained from the owner of the tamarins for publication of this report and any companying images.

Declaration of competing interest

The authors declare no conflict of interest.

References

Bochkov, A.V., 2009. A review of mites of the parvorder Eleutherengona (Acariformes: Prostigmata) – permanent parasites of mammals. Acarina (Supplement). KMK Scientific Press, Moscow, p. 149.

Brcko, I.C., Carneiro, J., Ruiz-García, M., Boubli, J.P., Silva-Júnior, J.S.E., Farias, I., Hrbek, T., Schneider, H., Sampaio, I., 2022. Phylogenetics and an updated taxonomic status of the tamarins (Callitrichinae, Cebidae). Mol. Phylogenet. Evol. 173, 107504.

Brosseau, G., 2020. Oral fluralaner as a treatment for *Demodex aurati* and *Demodex criceti* in a golden (Syrian) hamster (*Mesocricetus auratus*). Can. Vet. J. 61, 135–137.

Chen, W., Plewig, G., 2014. Human demodicosis: revisit and a proposed classification. Br. J. Dermatol. 170, 1219–1925.

Churgin, S.M., Lee, F.K., Groenvold, K., Kovi, R.C., Cheung, K.Y., Martelli, P.R., Zoo, C., 2018. Successful treatment of generalized demodicosis in red-handed tamarins (*Saguinus midas*) using a single administration of oral fluralaner. J. Zoo Wildl. Med. 49, 470–474.

Duangkaew, L., Hoffman, H., 2018. Efficacy of oral fluralaner for the treatment of *Demodex gatoi* in two shelter cats. Vet. Dermatol. 29, 262.

Gassel, M., Wolf, C., Noack, S., Williams, H., Ilg, T., 2014. The novel isoxazoline ectoparasiticide fluralaner: selective inhibition of arthropod γ-aminobutyric acid- and L-glutamate-gated chloride channels and insecticidal/acaricidal activity. Insect Biochem. Mol. Biol. 45, 111–124.

Gruber-Dujardin, E., Ludwig, C., Bleyer, M., Kaup, F.J., Mätz-Rensing, K., 2019. Cutaneous demodicosis and UV-induced skin neoplasia in two Goeldi's monkey (*Callimico goeldii*). J. Zoo Wildl. Med. 50, 470–473.

Hickey, T.E., Kelly, W.A., Sitzman, J.E., 1983. Demodectic mange in a tamarin (*Saguinus geoffroyi*). Lab. Anim. Sci. 33, 192–193.

Izdebska, J.N., Rolbiecki, L., 2020. The biodiversity of demodecid mites (Acariformes: Prostigmata), specific parasites of mammals with a global checklist and a new finding for *Demodex sciurinus*. Diversity 12, 261.

James, S.B., Raphael, B.L., 2000. Demodicosis in red-handed tamarins (*Saguinus midas*). J. Zoo Wildl. Med. 31, 251–254.

Karjala, Z., Desch, C.E., Starost, M.F., 2005. First description of a new species of *Demodex* (Acari: Demodecidae) from rhesus monkey. J. Med. Entomol. 42, 948–982.

Katoh, K., Standley, D.M., 2013. MAFFT multiple sequence alignment software version 7: improvements in performance and usability. Mol. Biol. Evol. 30, 772–780.

Kuznetsova, E., Vysokikh, A., Bourdeau, P., 2012. First description of demodicosis in 12 galagos (*Galago senegalensis*). Vet. Dermatol. 23, 61-e14.

Lebel, R.R., 1970. *Demodex saimiri* sp. nov. and *Demodex sciurei* sp. nov. ectoparasites of the squirrel mokey, *Saimiri sciureus*, with notes on demodicids from other subhuman primates. Master's Thesis, University Massachusetts, Amherst, MA, USA.

Lebel, R.R., Nutting, W.B., 1973. Demodectic mites of subhuman primates I: *Demodex saimiri* sp. n. (Acari: demodicidae) from the squirrel monkey, *Saimiri sciureus*. J. Parasitol. 59, 719–722.

Nutting, W.B., 1950. Stuides on the Genus *Demodex* Owen (Acari, Demodicoidea, Demodicidae). Ph.D. Thesis. Cornell University, Ithaca, NY, USA.

Nutting, W.B., 1964. Demodicidae – status and prognostics. Acarologia 6, 441–454.

Nutting, W.B., 1976. Hair follicle mites (*Demodex* spp.) of medical and veterinary concern. Cornell Vet. 66, 214–231.

Peddie, J.F., Larson, E.J., 1971. Demodectic acariasis in a woolly monkey. Vet. Med. Small Anim. Clin. 66, 485–488.

Palopoli, M.F., Fergus, D.J., Minot, S., Pei, D.T., Simison, W.B., Fernandez-Silva, I., Thoemmes, M.S., Dunn, R.R., Trautwein, M., 2015. Global divergence of the human follicle mite *Demodex folliculorum*: persistent associations between host ancestry and mite lineages. Proc. Natl. Acad. Sci. U.S.A. 112, 15958–15963.

Perego, R., Spada, E., Foppa, C., Proverbio, D., 2019. Critically appraised topic for the most effective and safe treatment for canine generalised demodicosis. BMC Vet. Res. 15, 17.

Phillipe, J., 1948. Note sur les gales du singe. Bull. Soc. Pathol. Exot. 41, 597–600.

Prasher, P., Baghra, D., Singh, D., Thakur, S., Gill, N.K., Kesavan, A.K., 2020. Molecular identification and phylogenetic relationship of *Demodex* mites based on mitochondrial 16S rDNA. Tropenmed. Parasitol. 10, 136–141.

Sastre, N., Ravera, I., Villanueva, S., Altet, L., Bardagí, M., Sánchez, A., Francino, O., Ferrer, L., 2012. Phylogenetic relationships in three species of canine *Demodex* mite based on partial sequences of mitochondrial 16S rDNA. Vet. Dermatol. 23, 509-e101.

Sastre, N., Francino, O., Curti, J.N., Armenta, T.C., Fraser, D.L., Kelly, R.M., Hunt, E., Silbermayr, K., Zewe, C., Sánchez, A., Ferrer, L., 2016. Detection, prevalence and phylogenetic relationships of *Demodex* spp. and further skin Prostigmata mites (Acari, Arachnida) in wild and domestic mammals. PLoS One 11, e0165765.

Tamura, K., Stecher, G., Kumar, S., 2021. MEGA11: molecular evolutionary genetics analysis version 11. Mol. Biol. Evol. 38, 3022–3027.

Thoemmes, M.S., Fergus, D.J., Urban, J., Trautwein, M., Dunn, R.R., 2014. Ubiquity and diversity of human-associated *Demodex* mites. PLoS One 9, e106265.

Wilson, N., Dietz, J.M., Whitaker Jr., J.O., 1989. Ectoparasitic acari found on golden lion tamarins (*Leontopithecus rosalia rosalia*) from Brazil. J. Wildl. Dis. 25, 433–435.